Structural and Kinetic Analysis of the Chemical Rescue of the Proton Transfer Function of Carbonic Anhydrase II[†]

David Duda,[‡] Chingkuang Tu,[§] Minzhang Qian,[§] Philip Laipis,[‡] Mavis Agbandje-McKenna,[‡] David N. Silverman,*[,§] and Robert McKenna*[,‡]

Department of Biochemistry and Molecular Biology and Department of Pharmacology and Therapeutics, University of Florida, Gainesville, Florida 32610

Received October 2, 2000; Revised Manuscript Received November 24, 2000

ABSTRACT: Histidine 64 in human carbonic anhydrase II (HCA II) functions in the catalytic pathway of CO_2 hydration as a shuttle to transfer protons between the zinc-bound water and bulk water. Catalysis of the exchange of ^{18}O between CO_2 and water, measured by mass spectrometry, is dependent on this proton transfer and was decreased more than 10-fold for H64A HCA II compared with wild-type HCA II. The loss of catalytic activity of H64A HCA II could be rescued by 4-methylimidazole (4-MI), an exogenous proton donor, in a saturable process with a maximum activity of 40% of wild-type HCA II. The crystal structure of the rescued complex at 1.6 Å resolution shows 4-MI bound in the active-site cavity of H64A HCA II, through π stacking interactions with Trp 5 and H-bonding interactions with water molecules. In this location, 4-MI is about 12 Å from the zinc and approximates the observed "out" position of His 64 in the structure of the wild-type enzyme. 4-MI appears to compensate for the absence of His 64 and rescues the catalytic activity of the H64A HCA II mutant. This result strongly suggests that the out conformation of His 64 is effective in the transfer of protons between the zinc-bound solvent molecule and solution.

Carbonic anhydrase II, one of the most efficient isozymes in the α class of carbonic anhydrases (*1*), catalyzes the hydration of CO_2 in two stages (*2*, *3*). The first is the conversion of CO_2 into bicarbonate by reaction with a zinc-bound hydroxide; the dissociation of bicarbonate leaves a water molecule at the zinc (eq 1)

$$CO_2 + EZnOH^- \rightleftharpoons EZnHCO_3^- \overset{[H_2O]}{\rightleftharpoons} EZnH_2O + HCO_3^- \quad (1)$$

$$EZnH_2O + B \rightleftharpoons EZnOH^- + BH^+ \quad (2)$$

The second step is the transfer of a proton to solution to regenerate the zinc-bound hydroxide (eq 2); here B denotes a proton acceptor, either an exogenous proton acceptor from solution or a residue of the enzyme itself, although ultimately the proton must be transported to solution. A number of studies have shown that His 64 in human carbonic anhydrase II (HCA II)[1] functions as a proton acceptor/donor in the shuttling pathway (*2*, *4*, *5*). The three-dimensional structure of wild-type HCA II at pH 8.5 shows His 64 located in the active-site cavity with its imidazole ring in the "in" conformation, approximately 7 Å from the zinc ion (*6*). The position of His 64 and its distance from the zinc ion suggests that proton-transfer proceeds through intervening hydrogen-bonded water bridges. However, although many such water molecules are in the active-site cavity of the HCA II crystal structure, a complete hydrogen-bonding pathway between His 64 and the zinc-bound water is not evident in the structure (*3*, *6*).

An observation that established the function of His 64 in the proton transport pathway was the reduction in catalysis by a site-specific mutant of HCA II in which His 64 is replaced by Ala (H64A HCA II),[1] a residue which does not support proton transport. The turnover number for catalysis, k_{cat}, of CO_2 hydration by H64A HCA II was decreased approximately 10-fold compared to the wild-type enzyme. The decrease in catalysis could be rescued in a saturable manner by the addition of exogenous proton acceptor/donors in solution, such as imidazole and its derivatives (*5*). It has been an intriguing observation that the chemical rescue of H64A HCA II by small exogenous compounds is substantial, with catalysis at saturation levels of additives approaching that of wild-type HCA II (*5*). This suggests that useful information about proton transport in carbonic anhydrase

[†] This work was supported by grants from the National Institutes of Health GM25154 (D.N.S.) and the University of Florida, College of Medicine start-up funds (R.M.).

* To whom correspondence should be addressed. (D.N.S.) Phone: (352) 392-3556. Fax: (352) 392-9696. E-mail: silvermn@college.med.ufl.edu. (R.M.) Phone (352) 393-5696. Fax: (352) 392-3422. E-mail: rmckenna@ufl.edu.

[‡] Department of Biochemistry and Molecular Biology, University of Florida College of Medicine, Gainesville, FL 32610-0245.

[§] Department of Pharmacology and Therapeutics, University of Florida College of Medicine, Gainesville, FL 32610-0267.

[1] Abbreviations: HCA II, human carbonic anhydrase II; H64A HCA II, the site-specific mutant of human carbonic anhydrase II containing the replacement of His64 with Ala; 4-MI, 4-methylimidazole; rms, root-mean-square; R_1/[E] is a rate constant for the interconversion of CO_2 and bicarbonate catalyzed by carbonic anhydrase as shown in eq 3; R_{H_2O}/[E] is a rate constant for the proton-transfer-dependent release of ^{18}O-labeled water from the active site of carbonic anhydrase shown in eq 4.

10.1021/bi002295z CCC: $20.00
Published on Web 01/17/2001

could be obtained by careful kinetic analysis of the extent of activation of H64A HCA II by exogenous proton acceptor/donors, and by structural localization of the binding sites of these exogenous agents.

We have compared the catalytic properties of H64A HCA II with and without the exogenous proton acceptor/donor 4-methylimidazole (4-MI)[1] to wild-type HCA II. To observe the effect of 4-MI binding on catalysis, we measured the exchange of ^{18}O between CO_2 and water at chemical equilibrium. We found that the enhancement of activity caused by addition of 4-MI to H64A HCA II was saturable with a maximum rate that approached that of the wild-type enzyme. Structural studies of 4-MI bound to H64A HCA II provided an explanation of this response. The crystal structure shows that this alternate proton acceptor binds to the enzyme in close proximity to the now vacant position previously occupied by the imidazole ring of His 64 in the wild-type enzyme structure. The rescue occurs due to positional substitution of 4-MI for His 64. These studies add to our understanding of proton-transfer processes in carbonic anhydrase.

MATERIALS AND METHODS

Enzymes. Wild-type HCA II and H64A HCA II were prepared and expressed in *Escherichia coli* as previously described (*5*, *7*) and were purified by affinity chromatography (*8*). The sequences of both enzymes were confirmed by sequencing the DNA of the entire coding region for carbonic anhydrase in the expression vector. Concentrations of human carbonic anhydrases were determined from the molar absorptivity at 280 nm (5.5×10^4 M^{-1} cm^{-1}) and were also determined by titration with the tight-binding inhibitor ethoxzolamide (*9*); these measurements gave results in close agreement.

Crystallography. Crystals of H64A HCA II were produced by the hanging drop method (*10*), using a 10 mg/mL isozyme solution in 50 mM Tris·HCl, pH 7.8, containing 1 mM $HgCl_2$. The drops were obtained by mixing 5 μL of the enzyme solution with 5 μL of precipitant solution. Each drop was equilibrated by vapor diffusion against 1 mL of precipitant solution at 4° C. The precipitant solution consisted of 2.3−2.5 M $(NH_4)_2SO_4$ in 50 mM Tris·HCl, pH 7.8, and 1 mM $HgCl_2$.

Crystals of H64A HCA II complexed with 4-MI were obtained by soaking H64A HCA II crystals in 50 mM Tris·HCl, pH 7.8, containing 3.0 M $(NH_4)_2SO_4$ and 0.5 M 4-MI. The crystals were kept in the soaking solution at 4° C for 1 week prior to data collection.

X-ray-diffraction data sets were collected using an R-AXIS IV++ image plate system with Osmic mirrors and a Riguku HU-H3R CU rotating anode operating at 50 kV and 100 mA. The data were collected using a 0.3 mm collimator with a detector to crystal distance of 100 mm and the 2θ angle fixed at 0°. The H64A HCA II data were collected at 300K using five crystals and the H64A HCA II 4-MI data were collected at 100 K using 1 crystal. All the frames were collected using a 1.0° oscillation angle with an exposure time of 600 s/frame.

A total of 113° of frames were collected from the five H64A HCA II crystals, with approximately 20 useful frames from each crystal. A total of 139 667 reflections were measured to a maximum resolution of 1.6 Å. The crystals belong to the $P2_1$ space group with unit cell parameters of $a = 42.5$, $b = 41.6$, $c = 72.7$ Å, and $\beta = 104.2°$. The data set was merged to a set of 27 019 independent reflections (82.6% complete) with the DENZO software and scaled with SCALEPACK (*11*), resulting in a $R_{sym} = 0.052$. The R_{sym} is defined as $R_{sym} = \sum [ABS(I - \langle I \rangle)]/\sum (I)$, where I is the intensity of an individual reflection and $\langle I \rangle$ is the average intensity for this reflection; the summation is over all intensities.

Table 1: Data Set Statistics for H64A HCA II in the Absence and Presence of 4-Methylimidazole (4-MI)

	H64A HCA II			H64A HCA II 4-MI		
resolution shells (Å)	no. of unique reflections	% data	linear *R*-factor	no. of unique reflections	% data	linear *R*-factor
25.00−3.44	2804	82.9	0.041	3097	94.0	0.034
3.44−2.74	2875	87.0	0.048	3140	96.6	0.039
2.74−2.39	2857	87.6	0.055	3057	95.4	0.049
2.39−2.17	2889	88.1	0.063	3009	94.1	0.052
2.17−2.02	2896	88.9	0.067	2974	93.6	0.057
2.02−1.90	2830	87.1	0.076	2930	91.9	0.063
1.90−1.80	2729	84.2	0.094	2858	89.8	0.076
1.80−1.72	2641	81.0	0.118	2767	86.7	0.084
1.72−1.66	2519	77.7	0.151	2599	81.7	0.099
1.66−1.60	1979	61.5	0.169	2018	64.1	0.107
Total	27019	82.6	0.052	28449	88.9	0.047

Due to observed crystal decay during the 300 K data collection of H64A HCA II, conditions for soaking the crystals in a cryoprotectant and collecting the data at 100 K using an Oxford cryocooling system were explored. A quick immersion of the crystals in a solution of 3.0 M $(NH_4)_2SO_4$, 30% glycerol in 50 mM Tris·HCl, pH 7.8, was found to be successful. A total of 330 frames of data were collected for a H64A HCA II crystal soaked with 4-MI under cryo conditions. A total of 468 251 reflections were measured to a maximum resolution of 1.6 Å. The crystal belongs to the $P2_1$ space group with unit cell parameters of $a = 42.1$, $b = 41.5$, $c = 72.1$ Å, and $\beta = 104.3°$. The data set was merged to a set of 28 456 independent reflections (88.8% complete) with the DENZO software and scaled with SCALEPACK (*11*), with an $R_{sym} = 0.047$.

The mosaicity of the data set collected for H64A HCA II soaked 4-MI collected at 100 K was high at 1.0° compared to that for H64A HCA II data set collected 300 K which had a mosaicity of between 0.3 and 0.6°. The unit cell volume of the mutant crystals soaked with 4-MI (122 066 $Å^3$) was 2% less than that of the mutant crystals alone (124 606 $Å^3$). The data set statistics are given Table 1.

Models of H64A HCA II with and without 4-MI were built using the program O, version 7 (*12*), and refined using the software package CNS, version 1.0 (*13*). The known structure of the wild-type HCA II isozyme (Protein Data Base accession number 2CBA), from which all the water molecules and the zinc atom had been removed, was used as the starting phasing model for both data sets (*14*). The initial maps were phased to 1.6 Å resolution. After one cycle of rigid body refinement followed by geometry-restrained positional refinement, the $(2|F_o| - |F_c|)$ and $(|F_o| - |F_c|)$ Fourier maps clearly showed the location of the Hg and zinc atoms as well as the 4-MI (in the data set of H64A HCA II soaked with 4-MI, although 4-MI had not been included in the model at this point). The ions were assigned to the models which were then further simulated, annealed, and refined by

Table 2: Refinement Statistics for H64A HCA II in the Absence and Presence of 4-Methylimidazole (4-MI)

	H64A HCA II	H64A HCA II 4-MI
R_{cryst}[a]	0.180	0.180
R_{free}[a]	0.200	0.204
no. of residues	3−261	3−261
no. of atoms	2057	2063
no. of H_2O molecules	211	317
rmsd for bond lengths (Å)[b]	0.005	0.005
rmsd for angles (deg)[b]	1.348	1.382
Ramachandran statistics (%)		
most favored regions	88.5	87.7
allowed regions	11.1	11.9
generously allowed regions	0	0.5(1)
disallowed regions	0.5(1)	0
B-factors (Å^2)		
avg main-chain atoms	16.66	8.45
avg side-chain atoms	19.69	9.91
solvent	33.04	22.01

[a] $R_{cryst} = \sum||F_o| - |F_c||/\sum|F_{obs}|$, R_{free} is identical to R_{cryst} for data omitted from refinement (4.3% reflections with-held for H64A HCAII 4-MI, 4.0% reflections withheld for H64A HCAII). [b] rmsd = root-mean-square deviation. Ramachandran statistics were generated using the program Procheck (*25*).

heating to 3000 K and gradual cooling, followed by temperature factor refinement with CNS (*13*). The refinement of both structures continued independently as an iterative process with computer graphics molecular modeling, including the incorporation of 4-MI (in the soaked data set) and solvent molecules into the model to fit the calculated maps, prior to the next series of refinement cycles. Additional solvent molecules from subsequent cycles of refinement were localized using the automatic water picking program until the refinement converged for both models. Convergence was deemed as when no new solvent molecules could be placed in the model when examining a $(2|F_o| - |F_c|)$ map contoured at a 1.5σ level. Atomic temperature factors were refined isotropically. The rms error on atomic positions as estimated from Luzzati plots (*15*) was about 0.15 Å. The mean *B* values of the atoms in the H64A HCA II 4-MI (100 K) structure were 50% of the *B* values for the atoms in the H64A HCA II (300K) structure. One hundred and six more solvent molecules could be assigned in the H64A HCA II 4-MI structure compared to the H64A HCA II structure. The refinement statistics are given in Table 2. The coordinates have been deposited with the Protein Data Bank. The accession numbers are 1G0E and 1G0F for H64A HCA II with and without 4-MI, respectively.

Comparison of H64A HCA II with and without 4-MI and the wild-type HCA II isozyme (*14*) was conducted after a superimposition of the main-chain atoms using a least-squares fit (*13*).

Oxygen-18 Exchange. This method is based on the measurement by membrane-inlet mass spectrometry of the exchange of ^{18}O between CO_2 and water at chemical equilibrium (eqs 3 and 4).

$$HCOO^{18}O^- + EZnH_2O \rightleftharpoons EZnHCOO^{18}O^- \rightleftharpoons COO + EZnO^{18}H^- \quad (3)$$

$$EZnO^{18}H^- + BH^+ \rightleftharpoons EZnH_2{}^{18}O + B \rightleftharpoons EZnH_2O + H_2{}^{18}O + B \quad (4)$$

The kinetic equations for the redistribution of ^{18}O from the $CO_2-HCO_3^-$ system to water were solved to obtain two rates for the ^{18}O exchange catalyzed by carbonic anhydrase (*16*). The first is R_1 the rate of exchange of CO_2 and HCO_3^- at chemical equilibrium, as shown in eq 3 and described by eq 5.

$$R_1/[E] = k_{cat}^{ex}[S]/(K_{eff}^{s} + [S]) \quad (5)$$

Here k_{cat}^{ex} is a rate constant for maximal interconversion of substrate and product, K_{eff}^{s} is an apparent binding constant for substrate to enzyme, and [S] is the concentration of substrate taken as CO_2 in this work. The ratio k_{cat}^{ex}/K_{eff}^{s} is, in theory and in practice, equal to k_{cat}/K_m for hydration obtained by steady-state methods. The binding of CO_2 to the active site of carbonic anhydrase is weak (*17*), and in this work $[CO_2] \ll K_{eff}^{s}$ so we are able to obtain k_{cat}/K_m from the ^{18}O exchange data. This was confirmed for H64A HCA II by measurement of the substrate dependence of ^{18}O exchange and by direct comparisons of k_{cat}^{ex}/K_{eff}^{s} determined by ^{18}O exchange and k_{cat}/K_m determined by stopped-flow.

A second rate determined by the ^{18}O exchange method is R_{H_2O}, the proton-transfer-dependent rate of release from the enzyme of water bearing substrate oxygen (eq 4). This is the component of the ^{18}O exchange that is enhanced by exogenous proton donors (*16*). In such enhancements, the exogenous donor acts as a second substrate in the catalysis providing a proton (eq 4), and the resulting effect on ^{18}O exchange is described by eq 6 below. This expression describes the approach of $R_{H_2O}/[E]$ to saturation as dependent on the formation of a bound complex between the exogenous donor and the enzyme.

$$R_{H_2O}/[E] = k_B^{obs}[B]/(K_{eff}^{B} + [B]) + R_{H_2O}{}^0/[E] \quad (6)$$

Here k_B^{obs} is the observed maximal rate constant for the release of $H_2{}^{18}O$ to bulk water caused by the addition of the buffer. K_{eff}^{B} is an apparent binding constant of the buffer to the enzyme, [E] and [B] are the concentrations of total enzyme and total buffer, and $R_{H_2O}{}^0$ is the rate of release of $H_2{}^{18}O$ into solvent water in the absence of buffer and represents the contribution to proton transfer from other sites on the enzyme or possibly solvent water itself.

The pH dependence of k_B^{obs} is often bell shaped, consistent with the transfer of a proton from a single predominant donor to the zinc-bound hydroxide. In these cases the pH profile is adequately fit by eq 7 in which k_B is a maximal, pH independent rate constant for proton transfer, K_B is the ionization constant of the proton donor BH^+ of eq 4, and K_E is the ionization constant of the zinc-bound water.

$$k_B^{obs} = k_B/\{(1 + K_B/[H^+])(1 + [H^+]/K_E)\} \quad (7)$$

Measurement of the isotopic content of CO_2 was made with an Extrel EXM-200 mass spectrometer with a membrane-inlet probe (*16*). Solutions contained 25 mM total concentration of all species of CO_2 unless otherwise indicated. Total ionic strength of solution was maintained at a minimum of 0.2 M by addition of Na_2SO_4.

RESULTS

Structure. The overall three-dimensional structures of H64A HCA II with and without 4-MI are very similar to

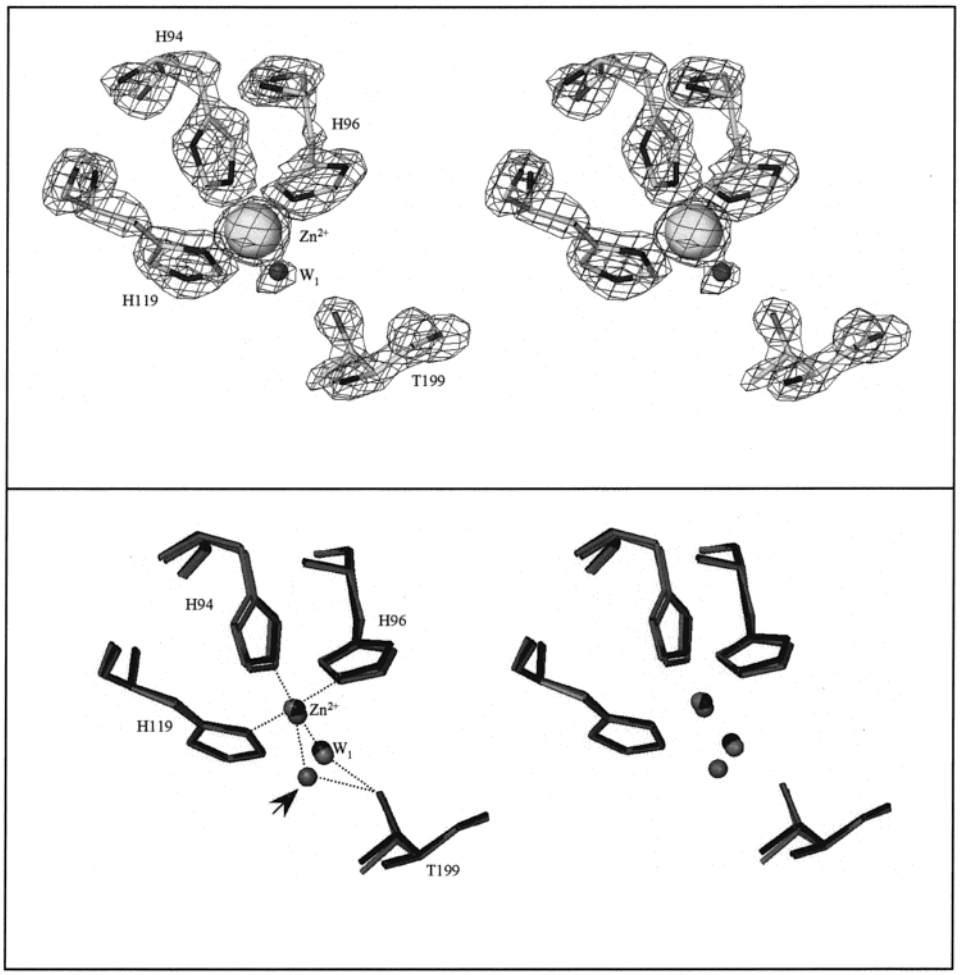

FIGURE 1: Tetrahedral coordination of zinc in the active site of HCA II. Stereoviews of (top) $2|F_o| - |F_c|$ electron density map of H64A HCA II complexed with 4-methylimidazole (4-MI) showing the coordination of the zinc ion with the water/hydroxide bound (w_1) (Table 3). Shown are residues His 94, 96, and 119 that coordinate the zinc ion and Thr 199, a hydrogen bond acceptor for the protonated solvent ligand of the zinc ion (*6*, *26*). Least squares superimposition (bottom) of H64A HCA II with 4-MI (black) and without 4-MI (dark gray), and wild-type HCA II (14) (light gray). The 4-MI bound and wild-type structures show the tetrahedral coordination of the zinc. The H64A HCA II without 4-MI (dark gray) shows a displacement of the bound water/hydroxide (indicated by an arrow). Hydrogen bond interactions are depicted as dashed lines.

that of other published HCA II structures. A least-squares fit of the structures of H64A HCA II with and without 4-MI to HCA II (*14*) gave an rms deviation for the Cα atoms of 0.274 and 0.321 Å, respectively. The wild-type HCA II structure by Håkansson et al. (*14*) was used for all comparative measurements because it was determined to a similar of resolution (1.54 Å) and at a comparable pH (7.8) to the structures determined in this paper.

In the wild-type HCA II isozyme structure (*14*) the zinc coordination polyhedron is a regular tetrahedron with three histidine nitrogens (His94, Nϵ2; His96, Nϵ2; His 119, Nδ1) and a water/hydroxide molecule as a ligand (Figure 1, top, Table 3). Comparison of the coordination geometry about the zinc ion in H64A HCA II showed an indirect effect of the replacement of His 64 with Ala on the water/hydroxide ligand to the zinc ion. In H64A HCA II the water/hydroxide molecule is significantly displaced from the zinc ion (2.27 Å) compared with that found in the wild-type enzyme structure (2.05 Å) and the regular tetrahedron coordination is disrupted (Table 3). In the H64A HCA II structure with bound 4-MI the water/hydroxide displacement is restored, the water/hydroxide molecule is brought closer to the zinc ion (1.81 Å), and the regular tetrahedral coordination of the zinc returned to that found in the wild-type enzyme structure (Figure 1, bottom).

Comparison of the electron density maps of H64A HCAII with and without 4-MI showed no detectable binding of 4-MI to the zinc ion. However, a single 4-MI molecule was bound near the entrance of the active-site cavity (Figure 2). This 4-MI has no hydrogen bond interactions with residues in the H64A HCA II structure; its is stabilized through π stacking interactions of the imidazole ring with the indole ring of Trp 5 which is approximately 4 Å away (Figure 3). The positions of Nδ1 and Nϵ2, the proton accepting/donating nitrogens of His 64, are 7.45 and 9.05 Å from the zinc ion in the in conformation and 10.46 and 12.11 Å from the zinc in the "out" conformation, respectively, in the structure of wild-type HCA II (*14*). In comparison, the functionally equivalent nitrogens, N1 and N3, of 4-MI are 13.44 and 12.01 Å from the zinc ion, respectively. The 4-MI is located close to the out conformation of His 64 in the structure of wild-type HCA II (*14*) and does not overlap with the position of His 64 in the in conformation, which is occupied by a water molecule in the H64A HCA II 4-MI structure.

Many plausible pathways for proton transfer from the zinc-bound water to the bulk solvent can be assigned along

Table 3: Coordination Geometries and Distances for Wild-Type HCA II and H64A HCA II in the Absence and Presence of 4-Methylimidazole (4-MI)

	active-site distances (Å)		
	HCA II	H64A HCA II	H64A HCA II 4-MI
Zn−His94 (Nϵ2)	2.10	2.10	2.13
Zn−His96 (Nϵ2)	2.12	2.09	2.03
Zn−His119 (Nδ4)	2.11	2.06	2.09
Zn−H_2O	2.05	2.27	1.81
Thr 199(Oγ1)−H_2O	3.94	3.52	3.60
	active-site angles (deg)		
	HCA II	H64A HCA II	H64A HCA II 4-MI
His94 (Nϵ2)−Zn−His96 (Nϵ2)	103.92	103.4	103.77
His94 (Nϵ2)−Zn−His119 (Nδ1)	115.32	112.77	113.83
His96 (Nϵ2)−Zn−His119 (Nδ1)	99.17	99.89	100.54
His94 (Nϵ2)−Zn−H_2O	111.06	108.08	106.77
His96 (Nϵ2)−Zn−H_2O	113.6	130.57	115.78
His119 (Nδ1)−Zn−H_2O	112.94	101.77	115.70
Thr 199(Oγ1)−H_2O−Zn	106.54	83.97	108.14
	Hg site distances (Å)		
	HCA II	H64A HCA II	H64A HCA II 4-MI
Cys 206 (Sγ)−Hg		2.21	2.28
Hg−H_2O (1)		2.36	2.43
Hg−H_2O (2)		3.12	−
Hg−Gln 137 O		2.87	2.85
Hg−Glu 205 O		3.15	3.19
	Hg site angles (deg)		
	HCA II	H64A HCA II	H64A HCA II 4-MI
Cys 206 (Sγ)−Hg−$H_2O_{(1)}$		177.26	179.52
Cys 206 (Sγ)−Hg−$H_2O_{(2)}$		86.64	
Cys 206 (Sγ)−Hg−Gln 137 O		91.01	93.49
Cys 206 (Sγ)−Hg−Glu 205 O		87.38	88.48
Gln 137 O−Hg−$H_2O_{(1)}$		89.62	86.03
Glu 205 O−Hg−$H_2O_{(1)}$		89.92	91.59
Glu 205 O−Hg−Gln 137 O		96.76	91.72
Gln 137 O−Hg−$H_2O_{(2)}$		145.56	
Glu 205 O−Hg−$H_2O_{(2)}$		117.41	
H_2O (1)−Hg−$H_2O_{(2)}$		94.34	
	Cys 206 χ1 Angle (deg)		
	HCA II	H64A HCA II	H64A HCA II 4-MI
Cys 206	63	−23	−13

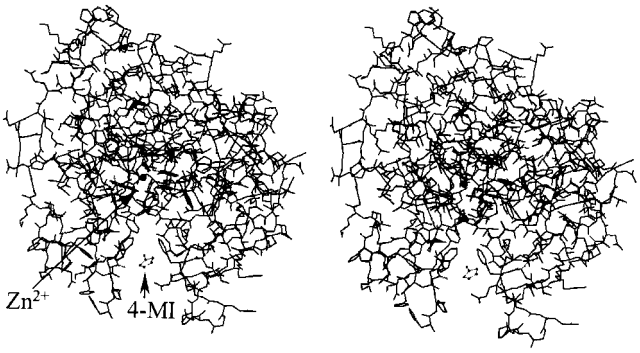

FIGURE 2: Stereoview stick diagram of H64A HCA II showing the location of the bound 4-methylimidazole (4-MI) in the active-site cleft. Arrows indicate the location of the zinc ion and 4-MI.

different water molecules in the active-site cavity of the structures of wild-type HCA II (*14*), H64A HCA II, and H64A HCA II 4-MI. However, the number of molecules utilized differs. In the wild-type structure (*14*), three water molecules (assigned 263, 318, and 292) form the network from the zinc ion to the Nδ1 nitrogen of His 64 in the in

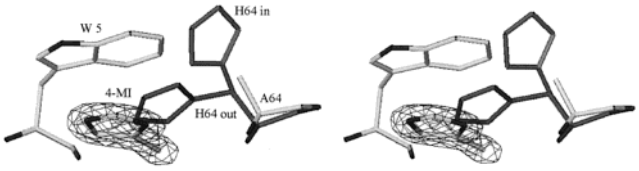

FIGURE 3: Stereoview of the bound 4-methylimidazole (4-MI). Shown is the $2|F_o| - |F_c|$ electron density map of 4-MI in relation to residues Trp 5 and Ala 64 of H64A HCA II. The 4-MI binds in the active-site cavity through a π stacking interaction of the imidazole ring with the indole ring of Trp 5. Also shown is the least-squares superimposition of the in and out conformations of His64 in the wild-type HCA II structure (14) (black).

conformation. However, in the H64A HCA II soaked with 4-MI, four water molecules (assigned 574, 394, 387, and 388) form this network to the N3 nitrogen of the 4-MI. The water molecule assigned 388 is located at the position where the Nδ1 nitrogen of His 64 is situated in the wild-type enzyme structure. An equivalent water molecule assigned 322 can also be seen in the structure of H64A HCA II without 4-MI, although the solvent leading out of the active-site cavity to the bulk solvent is different.

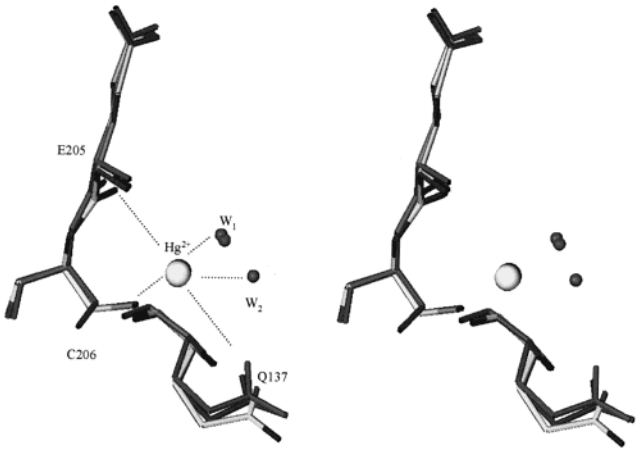

FIGURE 4: Stereoview of the linear coordination of the mercury ion in H64A HCA II with and without 4-methylimidazole (Table 3). Shown is the linear coordination of the Hg^{2+} by the Sγ sulfur of residue Cys 206 and water (w_1). There are further electrostatic interactions with the carbonyl oxygens of Gln 137 and Glu 205, and water (w_2) (Table 3). Also shown is a least squares superimposition of the wild-type HCA II structure (*14*) (black). Note residue Cys 206 in the wild-type HCA II (14) was crystallized in the absence of mercury ions and points away from the binding site.

The structures of H64A HCA II with and without 4-MI were crystallized in the presence of 1 mM $HgCl_2$, because mercuric and organomercury compounds are known to enhance HCA II crystal quality (*18*). The mercury ion was found to bind on the surface of H64A HCA II to the Sγ sulfur of Cys 206 and a water (assigned 432 in H64A HCA II, and 271 in H64A HCA II 4-MI) in a manner similar to that of other published HCA II structures. This caused the Cys 206 (χ1) in H64A HCA II to change conformation from that of the wild-type isozyme structure (*14*) enabling the Sγ sulfur of Cys 206 and a water molecule (assigned 432 in H64A HCA II and 271 in H64A HCA II 4-MI) to ligand the Hg^{2+} ion (Table 3, Figure 4). Other electrostatic interactions with the mercury ion include that with the carbonyl oxygen of Gln 137, Glu 205, and a second water molecule (assigned 389) in the structure of H64A HCA II without 4-MI.

Catalysis. R_{H_2O}/[E] is the rate constant for the proton-transfer-dependent release of $H_2$18O from the enzyme (eq 4). In the absence of 4-MI, R_{H_2O}/[E] was lower by 5-fold for H64A HCA II compared with wild-type at pH 7.7 (Figure 5). The addition of 4-MI resulted in the increase of R_{H_2O}/[E] for H64A HCA II in a saturable manner to a maximal level that was approximately equivalent to that of wild-type in the absence of 4-MI (Figure 5). Wild-type HCA II was activated by 4-MI by approximately 50% and showed evidence of inhibition at higher concentrations (Figure 5). This inhibition with increasing concentration of 4-MI was also evident as a decrease in R_1/[E] for both wild-type HCA II and H64A HCA II; however, in this case R_1/[E] was identical for both enzymes (Figure 5).

The pH profile of R_{H_2O}/[E] catalyzed by HCA II was bell-shaped and can be described using eq 7 in terms of a predominant proton donor to the zinc-bound hydroxide (*19*) (Figure 6). This proton donor has previously been identified as His 64 (5). The values obtained by a fit of eq 7 to these data give k_B, the rate constant for proton transfer to the zinc-bound hydroxide, of 8×10^5 s^{-1} for wild-type in the absence

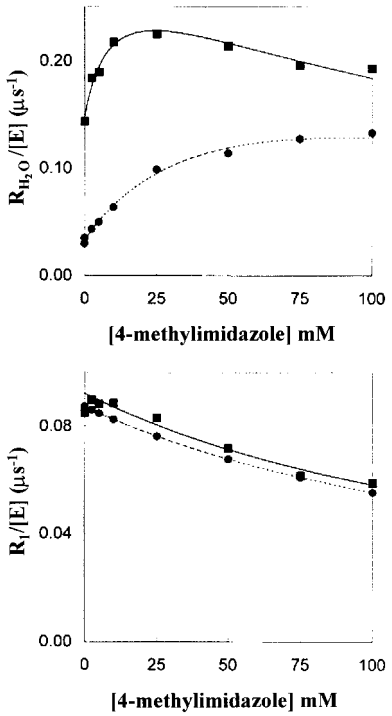

FIGURE 5: Variation with concentration of 4-methylimidazole (4-MI) of R_{H_2O}/[E] (*Top*) and R_1/[E] (bottom) determined from the catalysis of ^{18}O exchange by (■) wild-type HCA II, and (●) H64A HCA II at pH 7.7 and 25 °C. Solutions contained 25 mM total concentration of all species of CO_2 at 25 °C. The total ionic strength of solution was maintained at a minimum of 0.2 M by the addition of Na_2SO_4. The dashed line for R_{H_2O}/[E] catalyzed by H64A HCA II is a least-squares fit to eq 6 which gives K_{eff}^B near 20 mM (inhibition by 4-MI was neglected in this fit).

of 4-MI (Table 4). R_{H_2O}/[E] for H64A HCA II in the absence of 4-MI is considerably lower over nearly all of the pH range of Figure 6, except at the extremes; at pH near 7, R_{H_2O}/[E] is about 10-fold smaller than that for wild-type HCA II. The pH profile of H64A HCA II in the presence of 75 mM 4-MI is very similar to that of wild-type in the absence of 4-MI (Figure 6), with data from the fit to eq 7 given in Table 4. The value of k_B the rate constant for proton transfer from 4-MI to enzyme is 3×10^5 s^{-1}, about 40% of wild-type (Table 4). We obtained similar results for the steady-state turnover number, k_{cat}. At a saturating level of 4-MI (75 mM), catalysis of CO_2 hydration by H64A HCA II at pH 7.7 gave $k_{cat} = 4 \times 10^5$ s^{-1} (data not shown); for wild-type HCA II the value of k_{cat} at this pH is near 10^6 s^{-1} (*4*).

DISCUSSION

Catalysis of CO_2 hydration by carbonic anhydrase is activated by exogenous proton acceptor/donors to the zinc-bound water/hydroxide as shown in eq 2 (*2*). The maximal activation of catalysis by H64A HCA II caused by addition of imidazole and 1-methylimidazole approached the level of catalysis in wild-type HCA II (*5*). This is an intriguing result since the enhancement of catalysis by these exogenous molecules is free of the structural constraints of His 64 which functions as proton acceptor/donor in the shuttling pathway. It might be expected that exogenous imidazole would be able to enhance proton-transfer rates to an even greater extent by approaching the zinc ion in the active-site cavity more closely than does His 64. The apparent second-order rate

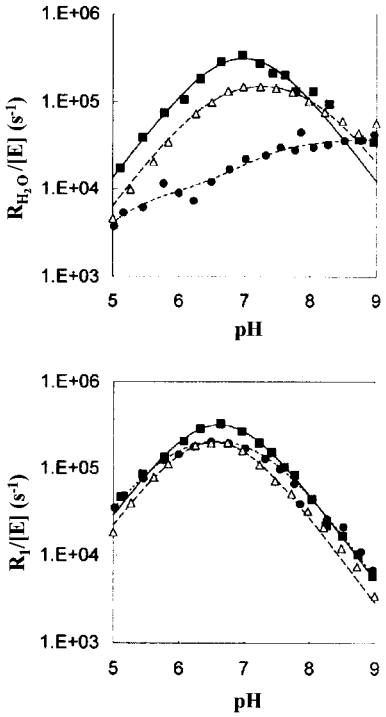

FIGURE 6: pH profile of R_{H_2O}/[E] (top) and R_1/[E] (bottom) determined from the catalysis of ^{18}O exchange by (■) wild-type HCA II in the absence of buffers, (●) H64A HCA II in the absence of buffers, and (△) H64A HCA II in the presence of 75 mM 4-methylimidazole. Other conditions as in Figure 5. The lines for wild-type and H64A HCA II are least-squares fits of eqs 5 and 7 with data given in Table 4.

Table 4: Ionization Constants and Maximal Values of Kinetic Constants for Human Wild-Type and H64A HCA II Obtained from Figures 5 and 6

	k_{cat}/K_m[a] ($\mu M^{-1}s^{-1}$)	pK_E[a]	k_B[b] (μs^{-1})	pK_B[b]	pK_E[b]
wild-type	98 ± 5	6.9 ± 0.1	0.8 ± 0.2	7.2 ± 0.3	6.8 ± 0.3
H64A	89 ± 4	7.5 ± 0.1	*c*	*c*	*c*
H64A + 75 mM 4-methylimidazole	87 ± 5	7.1 ± 0.1	0.30 ± 0.03	8.0 ± 0.2	6.5 ± 0.2

[a] Obtained from R_1/[E] by use of eq 5. [b] Obtained from R_{H_2O}/[E] by use of eq 7. [c] Data are complex indicating the presence of more than one proton donor.

constant k_{cat}/K_m for catalysis by H64A HCA II, if 4-MI is considered as second substrate, is $1 \times 10^7\ M^{-1}\ s^{-1}$ (obtained by applying the Michealis equation to the data for R_{H_20} in Figure 5), indicating a facile and near diffusion-controlled process. The rate constants k_{cat} and R_{H_2O}/[E] for catalysis by HCA II and H64A HCA II are determined predominantly by the proton-transfer steps between the zinc-bound solvent and His 64 or exogenous proton acceptor/buffers (*2*, *4*, *20*). R_{H_2O}/[E] is a rate constant for the proton-transfer-dependent release of ^{18}O-labeled water from the active-site of carbonic anhydrase shown in eq 4. Proton transfer is also a rate-limiting step for catalysis of CO_2 hydration by H64A HCA II enhanced by 4-MI; the turnover number k_{cat} for this enhancement has a solvent hydrogen isotope effect near 3 (*20*).

The observed activation of H64A HCA II catalysis by 4-MI was equivalent to catalysis by wild-type HCA II in the absence of 4-MI at pH 7.7 (Figure 5), and the rate constant for proton-transfer k_B between 4-MI and the zinc-bound hydroxide was 40% of wild-type (Table 4). In the wild-type HCA II structure, the position of His 64 at pH 8.5 is predominantly in the in conformation (*6*), while at a lower pH of 5.7, the conformation of His 64 is mainly in the out position (*21*). 4-MI binds in the active-site cavity of H64A HCA II near the position of His 64 in the out conformation in the wild-type enzyme structure (Figure 3). The distances between the zinc ion in the active-site cavity and the proton donating nitrogens of His 64 in the out conformation in the wild-type enzyme structure and of 4-MI bound to H64A HCA II are similar, 10.5 and 12.0 Å, respectively. Thus, the observation that the proton-transfer capability of 4-MI is very similar to that of His 64 in wild-type HCA II suggests that His 64 in the out position is a significant contributor to proton transfer in catalysis. This data is also consistent with results on catalysis by T200S HCA II, a mutant in which His 64 is predominantly in the out conformation and the maximal (or high pH) value of k_{cat} for CO_2 hydration is nearly identical with that found in wild-type HCA II (*22*).

The crystal structure of the complex of histamine bound to HCA II has been determined at pH 7.7−7.8 (*23*); it shows the imidazole ring of histamine forming hydrogen bonds with the side chains of Asn 62 and Gln 92 in the active-site cavity. In this structure the side chain of His 64 is in an in conformation. These observations do not preclude the possibility that the side-chain conformation of His 64 alternates between the out and in positions in transporting protons during catalysis.

The binding of 4-MI in the active-site cavity is rather weak. On the basis of the activation of R_{H_2O}/[E] shown in Figure 5, the value of the effective binding constant K^B_{eff} (eq 6) was close to 20 mM (inhibition by 4-MI was neglected in this fit). The pK_a of bound 4-MI in its productive mode, estimated using the pH profile of R_{H_2O}/[E], is 8.0 ± 0.2. This value is similar to the pK_a of 7.2 ± 0.3 determined for the imidazole ring of His 64 by the same method. These observations are consistent with the crystal structure in which 4-MI is bound in the active-site cavity, forming π stacking interactions with the indole ring of Trp 5 (Figure 3). There are no hydrogen-bonding interactions between 4-MI and other residues in mutant enzyme structure, although it does participate in hydrogen bonds with water molecules in the active-site cavity.

There are notable differences between the position of the bound 4-MI in H64A HCA II and the position of the imidazole ring of His 64 in the wild-type enzyme. The proton donating/accepting nitrogen in the bound 4-MI that is the nearest to the zinc ion in the active-site cavity is about 1.5 Å further away from the zinc ion than the functionally equivalent nitrogen in His 64 in the out conformation in the HCA II structure and 4.5 Å further away in the in conformation. These differences in distance may explain the somewhat lower value of k_B, a rate constant for the proton transfer, with bound 4-MI compared with wild-type enzyme (Table 4). In view of these positional differences, the observation that proton transfer proceeds very rapidly with bound 4-MI as with His 64 in the wild-type enzyme suggests that there is a large ensemble of proton-transfer pathways formed with different arrays of hydrogen-bonded water molecules that are able to extend to 4-MI in H64A HCAII as well as to the imidazole of His 64 in wild-type HCA II.

The position of bound 4-MI is similar to that of His 64 in the out position in the wild-type enzyme and does not overlap with the position of this residue in the in conformation in H64A HCA II 4-MI structure (Figure 3). This may be the basis of the observation (Figure 5) that 4-MI can also enhance catalysis by wild-type HCA II. It is possible that the 4-MI could occupy proximate locations to the in or out His 64 conformation positions in the wild-type HCA II if the His 64 is the converse conformation and can therefore participate in an additional proton-transfer pathway to that normally utilized by the wild-type enzyme. A comparison of the enhancement of catalysis for the wild-type and H64A HCA II enzymes shows that both have R_{H_2O}/[E] increased about 0.1 μs^{-1} at the maximum. However, this comparison is difficult because of the observed weak inhibition of both enzymes at higher levels of 4-MI (Figure 5). Although we have no direct data on the mode of this inhibition, it is possible that it is caused by the direct but very weak ligation of 4-MI to the zinc ion in a manner similar to the binding of imidazole to the zinc of HCA I (*24*).

Several changes in the active-site cavity are seen when His 64 is replaced with Ala, including an increase in the distance from the zinc to its fourth ligand, the bound solvent molecule. This difference is eliminated upon binding 4-MI. This effect may be due to a displacement of the equilibrium between zinc-bound water and zinc-bound hydroxide in the crystals (that is, a change in effective pH of the active site). The kinetic data indicate that there is no difference in chemistry at the zinc with and without His 64 because the values of the apparent pK_a of the zinc-bound water and of the maximal value of k_{cat}/K_m for hydration are very similar for H64A HCA II and wild-type HCA II (Table 4, Figure 6).

While it is not possible to discern whether the 4-MI is bound in the protonated or unprotonated form in the crystal structure of the complex with H64A HCA II at 1.6 Å resolution, the observation that the 4-MI occupies a position closely resembling that of His 64 in the out conformation may indicate that, like His 64 in the wild-type HCA II at lower pH, 4-MI is predominantly protonated. It is also important to note that the crystal structure of 4-MI bound to the mutant enzyme only gives an estimate of the proton-transfer pathway. The crystal structure of the complex at 1.6 Å resolution does not unambiguously show a completed, hydrogen-bonded pathway between the zinc-bound solvent molecule and bound 4-MI. A more detailed study of this problem using higher resolution diffraction data is now in progress.

The current study has outlined a novel approach to the study of proton-transfer pathways in proteins. For site-specific mutants in which proton shuttle residues have been replaced with nonionizable groups, a frequent observation is rescue by exogenous proton acceptor/donors. Identifying the site of binding of these exogenous molecules provides data that complements kinetic results and provides further information on the proton-transfer pathway in the wild-type enzyme. In the case of H64A HCA II, the crystal structure shows the exogenous acceptor/donor 4-MI forming a π stacking complex with Trp 5 and binding in a location close to that of His 64 in the out conformation in the wild-type HCA II structure, where the histidine side chain points away from the zinc ion in the active-site cavity and out into solution. This strongly suggests that this out conformation is effective in the transfer of protons between the zinc-bound solvent molecule and solution.

ACKNOWLEDGMENT

We thank Kris F. Tesh (Molecular Structure Corporation) for help in data X-ray diffraction data collection and Maria Kontou for helping install computer software. We also thank Joseph Gilboa (Weizmann Institute, Israel and visiting Professor at the University of Florida) and Lakshmanan Govindaswamy (University of Florida) for critical discussions.

REFERENCES

1. Hewett-Emmett, D., and Tashian, R. E. (1996) *Mol. Phylogenet. Evol. 5*, 50−77.
2. Lindskog, S. (1997) *Pharmacol. Ther. 74*, 1−20.
3. Christianson, D. W., and Fierke, C. A. (1996) *Acc. Chem. Res. 29*, 331−339.
4. Steiner, H., Jonsson, B.-H., and Lindskog, S. (1975) *Eur. J. Biochem. 59*, 253−259.
5. Tu, C. K., Silverman, D. N., Forsman, C., Jonsson, B. H., and Lindskog, S. (1989) *Biochemistry 28*, 7913−7918.
6. Eriksson, A. E., Jones, T. A., and Liljas, A. (1988) *Proteins: Struct., Funct., Genet. 4*, 274−282.
7. Tanhauser, S. M., Jewell, D. A., Tu, C. K., Silverman, D. N., Laipis, P. J. (1992) *Gene 117*, 113−117.
8. Khalifah, R. G., Strader, D. J., Bryant, S. H., and Gibson, S. M. (1977) *Biochemistry 16*, 2241−2247.
9. Segel, I. H. (1975) *Enzyme Kinetics*, pp 150−159, John Wiley & Sons, New York.
10. McPherson, A. (1982) *Preparation and analysis of protein crystals*, Wiley and Sons, New York.
11. Otwinowski, Z. (1992) *An oscillation data processing suite for macromolecular crystallography*, Yale University, New Haven, CT.
12. Jones, T. A., Zou, J.-Y., Cowan, S. W., and Kjeldgaard, M. (1991) *Acta Crystallogr., Sect. A 47*, 110−119.
13. Brunger, A. T., Adams, P. D., Core, G. M., Delano, W. L., Gross, P., Grosse-Kunstleve, R. W., Jiang, J.-S., Kuszewski, J., Nilges, N., Pannu, N. S., Read, R. J., Rice, L. M., Simonson, T., and Warren, G. L. (1998) *Acta Crystallogr., Sect. D 54*, 905−921
14. Hakansson, K., Carlsson, M., Svensson, L. A., and, Liljas, A. (1992) *J. Mol. Biol. 227*, 1192−1204.
15. Luzzati, V. (1952) *Acta Crystallogr. 5*, 802−810.
16. Silverman, D. N. (1982) *Methods Enzymol. 87*, 732−752.
17. Simonsson, I., Jonsson, B.-H., and Lindskog, S. (1979) *Eur. J. Biochem. 93*, 409−417.
18. Tilander, B., Strandberg, B., and Fridborg, K. (1965) *J. Mol. Biol. 12*, 740−760.
19. Silverman, D. N., Tu, C. K., Chen, X., Tanhauser, S. M., Kresge, A. J., and Laipis, P. J. (1993) *Biochemistry 32*, 10757−10762.
20. Taoka, S., Tu, C. K., Kistler, K. A., and Silverman, D. N. (1994) *J. Biol. Chem. 269*, 17988−17992.
21. Nair, S. K., and Christianson, D. W. (1991) *J. Am. Chem. Soc. 113*, 9455−9458.
22. Krebs, J. F., Fierke, C. A., Alexander, R. S., and Christianson, D. W. (1991) *Biochemistry 30*, 9153−9160.
23. Briganti, F., Mangani, S., Orioli, P., Scozzafava, A., Vernaglione, G., and Supuran, C. T. (1997) *Biochemistry 36*, 10384−10392.
24. Kannan, K. K., Petef, M., Fridborg, K., Cid-Dresdner, H., and Lovgren, S. (1977) *FEBS Lett. 73*, 115−119.
25. Laskowski, R. A., MacArthur, M. W., Moss, D. S., Thornton, J. M. (1993) *J. Appl. Crystallogr. 26*, 283−291.
26. Xue, Y., Liljas, A., Jonsson, B.-H., and Lindskog, S. (1993) *Proteins: Struct., Funct., Genet. 15*, 177−182.

BI002295Z